Continuous Optimal Infeed Control for Cylindrical Plunge Grinding, Part 2: Controller Design and Implementation

Shaoqiang Dong
Graduate Research Assistant

Kourosh Danai
Professor
e-mail: danai@ecs.umass.edu

Stephen Malkin
Distinguished Professor

Department of Mechanical and Industrial Engineering
University of Massachusetts Amherst

This is the second of two papers concerned with on-line optimization of cylindrical plunge grinding cycles with continuously varying infeed control. In the first paper [1], dynamic programming was applied to a simulation of the cylindrical grinding process in order to explore the characteristics of optimal grinding cycles. Optimal cycles were found to consist of distinct segments each with predominant constraints. An optimal control policy was formulated with the infeed rate within each segment determined according to the prevailing constraint. The present paper is concerned with the design of the controller and its implementation. The control system to implement the optimization policy is described together with provisions to enhance robustness to modeling uncertainty and measurement noise. Robustness provisions include model adaptation by parameter estimation from on-line measurements of size and power, and incorporation of safety margins in the optimization process. Problems associated with practical implementation of the control system, stemming from power limitations and wheel wear, are also discussed. The controller performance is demonstrated on an instrumented internal cylindrical grinding machine. [DOI: 10.1115/1.1751424]

1 Introduction

This paper and the previous one [1] explore the prospects for continuously varying infeed control of cylindrical plunge grinding cycles. As compared with conventional infeed cycles consisting of a few discrete stages with pre-specified infeed rates, continual variation of the controlled infeed rate could reduce the cycle time. In the previous paper [1], dynamic programming (DP) was applied to a simulation of the grinding process in order to investigate the characteristics of optimal infeed cycles with continuously variable infeed control. Optimal infeed control cycles were found to consist of distinct sections, similar to the stages in conventional cycles. The first section at the start of the grinding cycle uses the maximum allowable controlled infeed rate, similar to the roughing stage in the conventional cycle. The final section is at zero controlled infeed rate, similar to the conventional spark-out stage, to satisfy the roundness requirement. An intermediate section is also necessary, in most cases, where the infeed is varied so as to provide a balance between the depth of thermal damage (burn) and the remaining infeed. In the present paper, these characteristics are used for designing a controller and implementing optimal infeed control of the machine tool.

2 Controller Design

Implementation of the optimization policy requires a controller which can identify the state of the process at each sampling instant based on feedback measurements of size and power, and to determine the appropriate command infeed rate. This controller would use the process model to (1) compute the depth of burn at each sampling instant based on the measurements of power, (2) determine the actual infeed rate based on the past and current command infeed rates, (3) compute the command infeed rate to balance the depth of burn against the remaining infeed in the intermediate section based on the measurements of size, and (4) estimate the transients between the intermediate section and the last section. The controller performance will depend on the accuracy of the model and should be robust to model uncertainties. Some of this dependence was demonstrated in the previous paper [1] for different values of wheel dullness and system dynamics.

A schematic diagram of the proposed control system is shown in Fig. 1. The role of the block "Optimization" is to identify the state of the cycle using measurements of power and size and to compute the desired infeed rate v_d. Since the command infeed rate should be at its maximum allowable limit for the first section of the cycle and at zero for the last, the controller can be bypassed at these states. The actual infeed rate v is obtained on-line from size measurements, and values of the time constant τ and the effective wear flat area A_{eff} can be estimated in the block "Parameter Estimation" from measurements of power and size to add robustness to the control strategy.

Implementation of the states identified for the minimum-time cycles is as follows: The cycle starts at the maximum allowable infeed rate which is maintained either until the depth of thermal damage (burn) becomes equal to the remaining infeed, thereby triggering the start of the intermediate section, or until the remaining infeed indicates the beginning of the spark-out stage. The latter would happen if the wheel dressing is too coarse for thermal damage to occur [1]. This strategy implies that the depth of burn, if it occurs, needs to be estimated at each sampling instant based on power measurements to trigger the beginning of the intermediate section. For the intermediate section, the command infeed rate is computed so as to match the depth of burn to the remaining infeed. The time for switching to the final (spark-out) stage depends on the process dynamics. According to the model, at zero command infeed rate the actual infeed rate decreases exponentially:

$$v_i = v_{i-1} \exp(-\delta t/\tau) \tag{1}$$

and at the end of the cycle it should not exceed the final actual infeed rate v_f in order to satisfy the roundness constraint. The instant at which to switch to spark-out can therefore be deter-

Contributed by the Manufacturing Engineering Division for publication in the JOURNAL OF MANUFACTURING SCIENCE AND ENGINEERING. Manuscript received July 2003; Revised November 2003. Associate Editor: T. R. Kurfess.

 Copyright © 2004 by ASME

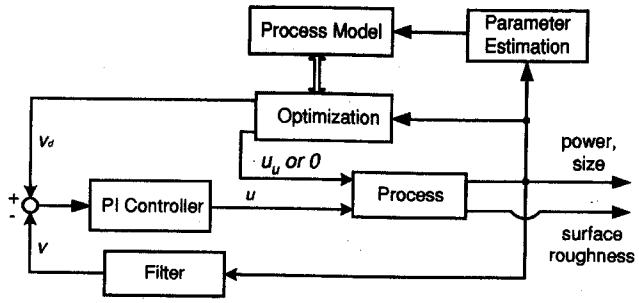

Fig. 1 Schematic diagram of the on-line control strategy

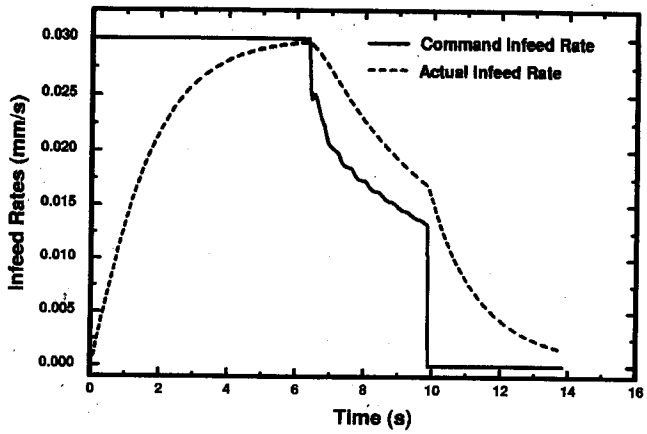

Fig. 2 Controlled infeed rate profile with simulated nonlinear process dynamics

mined by accounting for the time it takes for the current infeed rate v_k to decrease to v_f at zero command infeed rate. Using a first-order approximation, this time can be estimated as:

$$t_k = -\tau \log(v_f / v_k) \tag{2}$$

which leads to the depth of material to be removed during spark-out as:

$$q_k = \tau v_k (1 - \exp(-t_k/\tau)) \tag{3}$$

When the measured remaining infeed becomes equal to or less than q_k, the process will switch to the spark-out stage, and the wheel will be retracted when the size constraint is satisfied.

The proposed control system uses feedback to compensate for modeling uncertainty caused by parameter variations and external disturbances. Modeling uncertainty, which is manifested by mismatch between the blocks "Process Model" and "Process" in Fig. 1, may lead to constraint violations especially when the process is operated close to its optimal. One potential cause of mismatch is the linear time-invariant approximation for the system dynamics in the "Process Model." Linearity assumes that the normal grinding force is proportional to the actual infeed rate, but a slightly non-linear relationship is more likely [2]. In this study, a nonlinear normal force relationship was used in the simulation model representing the block "Process," whereas a first-order linear model was used to approximate the system dynamics in the block "Process Model." For simulation purposes, the instantaneous depth of cut a was calculated by simultaneously solving the infeed continuity equation and the normal force equation in terms of the depth of cut [3].

The performance of the on-line control system was evaluated in simulation for a Bryant Model No. 1116 Internal Grinder (later used for the experiments) with the nominal conditions used in computing the optimal cycles (see previous paper [1]) and a system stiffness of 8000 N/mm. The sampling period was set at 0.04 s, which gives significantly more steps than the dynamic programming (DP) solution. The command and actual infeed rates for this cycle in Fig. 2 are similar to the DP result. The optimality of the cycle can be better appreciated from the results for remaining infeed and depth of burn shown in Fig. 3. The depth of burn equals the remaining infeed from the end of the first section (6.4 s into the cycle) to the end of the cycle, verifying that the control system can successfully implement the optimization strategy imitated from the DP solution. The final estimated out-of-roundness for this cycle was 3.0 μm, which matched the specification.

Instead of allowing for workpiece burn with subsequent removal of the damaged material, a more conservative approach would be to completely avoid thermal damage throughout the cycle. In order to evaluate the performance of the controller with this more stringent requirement, the optimization policy was modified so as to match the grinding power to the threshold burning power within the intermediate section. The simulated infeed rates from this policy are shown in Fig. 4 with the corresponding grinding power and burning power in Fig. 5. These results strongly resemble the conventional three-stage cycle for the no-burn case. The cycle starts at the maximum infeed rate, similar to the roughing stage in the conventional cycle, but then proceeds to the second stage at a considerably lower infeed rate in order to avoid thermal damage. This more conservative policy lengthens the cycle time.

The control system will also need to cope with parametric uncertainty. For example, it has been assumed up to now that the effective wear flat area A_{eff} remains constant during the cycle. However, it is likely to progressively increase as the wheel wears

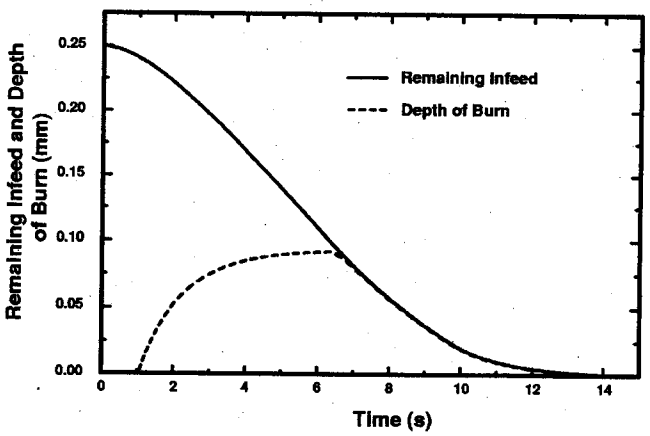

Fig. 3 Remaining controlled infeed and depth of burn with simulated nonlinear process dynamics

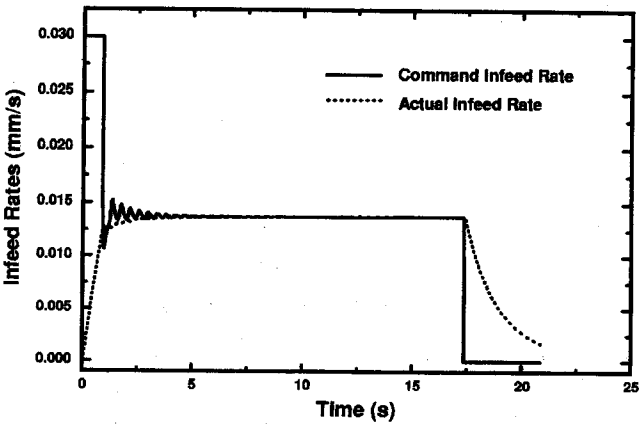

Fig. 4 Controlled infeed rate profile when thermal damage is not allowed

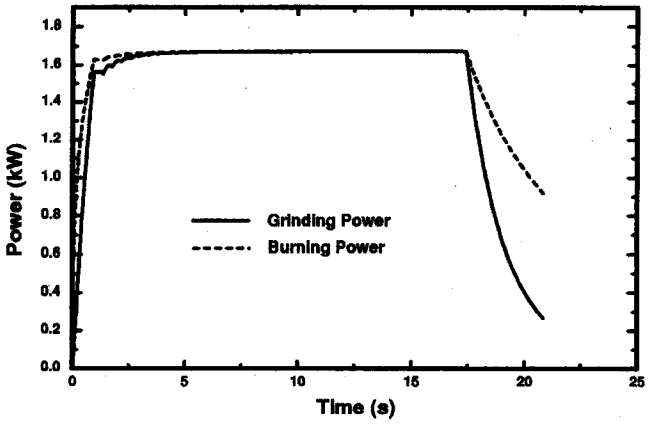

Fig. 5 Grinding power and burning power when thermal damage is not allowed

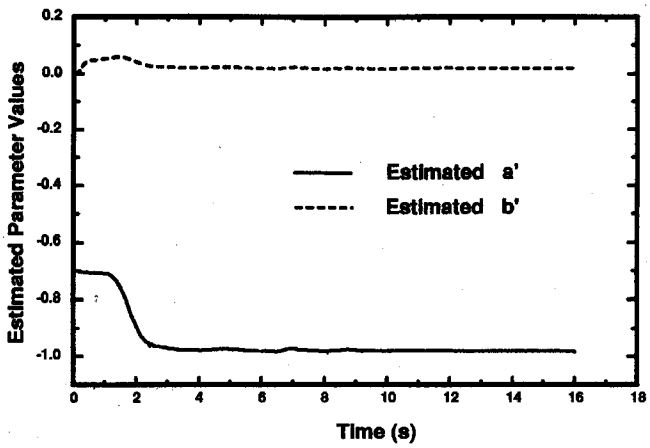

Fig. 7 Recursively estimated parameters of the first-order system dynamic model

[2]. The effect of allowing A_{eff} to increase from 0.026 to 0.032 during the optimal cycle, rather than remaining at its nominal value of 0.026, is shown in Fig. 6. The increasing A_{eff} results in a smaller actual infeed rate during the initial section, and a slightly longer cycle.

3 Implementation Issues

The performance of the control system depends upon the accuracy of the grinding model and estimation of variables from in-process measurements of size and power. For example, the value of the actual infeed rate is needed at each sampling instant to estimate the depth of burn and to determine when to switch to the spark-out stage. The actual infeed rate cannot be obtained by numerical differentiation, due to noise in the size measurements, so it needs to be estimated from the command infeed rate. In order to estimate the dynamics between the actual and command infeed rates, the counterpart first-order approximation between the measured infeed q and command infeed p can be used:

$$q(i)=a'q(i-1)+b'p(i-1) \tag{4}$$

where p and q are readily available, the parameters a' and b' can be estimated and then used in the identical relationship between the actual and command infeed rates

$$v(i)=a'v(i-1)+b'u(i-1) \tag{5}$$

to estimate the actual infeed rate from the values of the command infeed rate. The recursively estimated values of these two parameters from experimental size measurements using least-squares error estimation are shown in Fig. 7. Both parameters converge after about two seconds, which is well within the first section of the cycle. From the estimate of parameter a', the time constant of the system can then be estimated quickly enough to decide when to switch to the next section.

Another important parameter to be estimated is the effective wear flat area A_{eff}. Although A_{eff} can be approximated from the dressing parameters [2], it can be estimated more reliably from the sliding component of measured power which is proportional to the effective wear flat area

$$P_{sl}=0.842(d_e v)^{0.85}v_s A_{\text{eff}}/(n_w^{0.85}) \tag{6}$$

The variation of the estimated values of A_{eff} obtained from power measurements during a three-stage cycle, shown in Fig. 8, suggests the need for on-line estimation. But recursive estimation adds to the computational load and needs to be justified against the benefits of in-process model updates.

A possible alternative to on-line estimation is post-cycle adaptation, whereby the parameters are estimated off-line after each cycle to update the model for the subsequent cycle. To evaluate the utility of post-cycle adaptation for the wear flat area, the calculated power from the average value of the estimated A_{eff} is compared with the measured power for the three-stage cycle in Fig. 9. Since the measured and calculated power values match quite well, off-line estimation of A_{eff} should be a viable alternatives to on-line estimation. However, with post-cycle adaptation, the initial cycle will need to be operated with an approximate

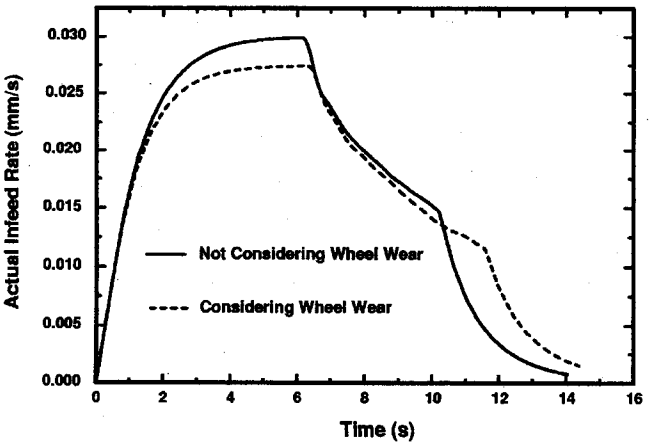

Fig. 6 Simulated actual infeed rate with and without wheel wear

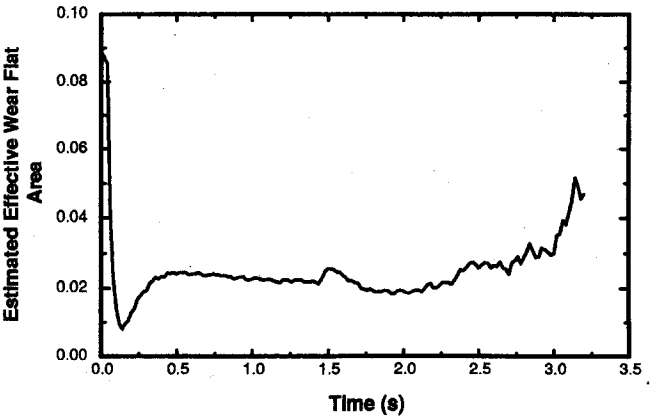

Fig. 8 Recursively estimated effective wear flat area from power measurements of a three-stage traditional cycle

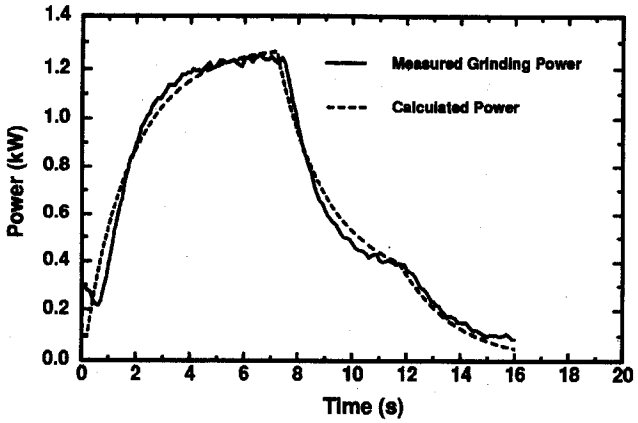

Fig. 9 Measured power and calculated power using the average estimate of the effective wear flat area

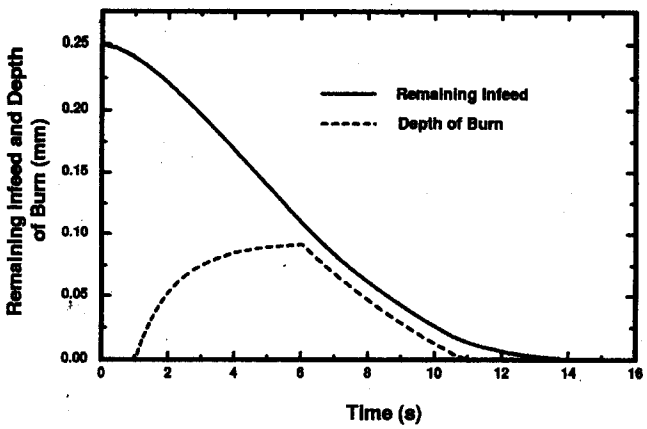

Fig. 11 Remaining infeed and depth of burn when a safety margin is included to compensate for an under-estimated effective wear flat area

value of the parameter until its estimate becomes available after the cycle. In this case, safeguards are needed to prevent erroneous estimates during the initial cycle. For example, the performance of the control system with A_{eff} less than its value in simulation by 10% is illustrated in Fig. 10. Under-estimation of A_{eff} resulted in an unacceptable part with a burned layer that is never completely removed.

As safeguard against modeling inaccuracies, such as those caused by an incorrect value of A_{eff}, a safety margin can be added to bias the equality between the depth of burn and remaining infeed during the intermediate section, as

$$z = q_r - m \tag{7}$$

where z denotes the depth of burn, q_r represents the remaining infeed and m denotes the safety margin. The safety margin ensures robustness to modeling uncertainty at the expense of efficiency. For example, inclusion of a safety margin for the failed cycle of Fig. 10 can result in a safe but sub-optimal cycle as shown in Fig. 11.

The safety margin can be reduced when there is more confidence in the model. For example, large safety margins incorporated in the initial cycle to ensure complete removal of the thermal damage may be reduced for subsequent cycles when a more accurate value of A_{eff} is available from post-cycle estimation. Reduction of the safety margin can be methodically performed by adopting the concept of Recursive Constraint Bounding (RCB) [5], where optimality is evaluated after the completion of each cycle according to the slack in each constraint. (Slack denotes the buffer between the measured or estimated variable and its constrained value.) Using this concept, the slack in the thermal damage constraint can be defined as the minimum distance $d(i)$ between the remaining infeed and depth of burn for the ith cycle, as

$$d(i) = \min\{\text{remaining}(j) - \text{burn}(j)\} \tag{8}$$

If $d(i)$ is positive and outside the noise buffer, the safety margin for the next cycle can be updated as

$$m(i+1) = m(i) - c[d(i) + n] \tag{9}$$

where $c \in [0,1]$ is the confidence level and n is the noise buffer used, respectively, to account for the level of modeling inaccuracy and noise associated with an actual constraint value.

Adaptation of the safety margin was studied in simulation with noisy power and size values. For this simulation, random numbers were added to the simulated values of size and power, and the actual infeed rate values were estimated from simulated noisy size values. Modeling inaccuracy was simulated by using an A_{eff} value in the controller 10% less than that used in the process simulation. The confidence level was selected as 0.25 and the noise buffer as 0.005 mm. The safety margin was initially set as 0.05 mm, and subsequently updated after each cycle based on the minimum distance between the remaining infeed and depth of burn during the cycle. The times for a series of cycles with adapted safety margins at a confidence level of 0.25, plotted in Fig. 12, show a reduction in cycle time from 15.7 s to 13.2 s in seven cycles, a savings of approximately 2.4 seconds. The thermal damage constraint be-

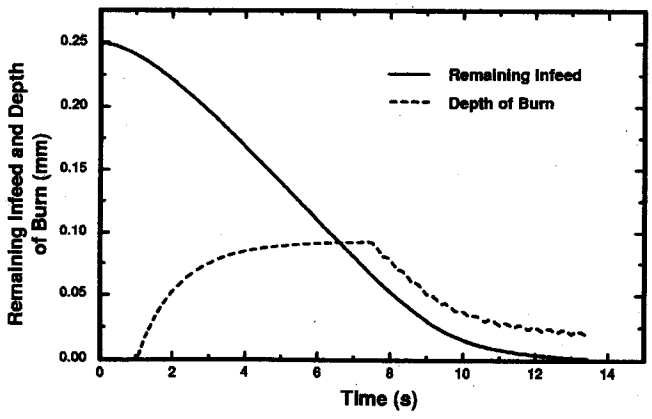

Fig. 10 Remaining infeed and depth of burn when the effective wear flat area is under-estimated

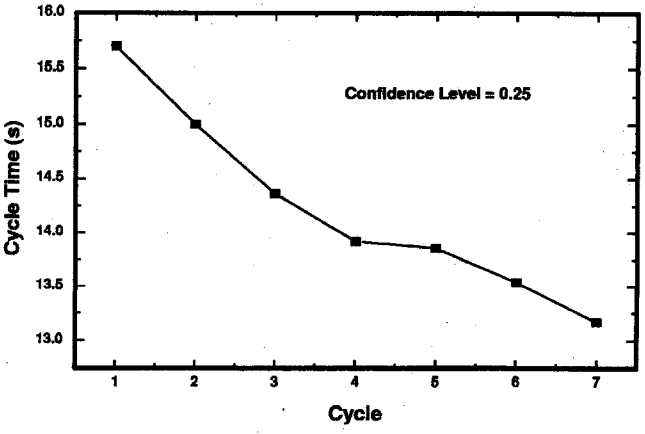

Fig. 12 Reduction of cycle time with an initial safety margin of 0.05 mm and a confidence level of 0.25 when wear flat area is under-estimated

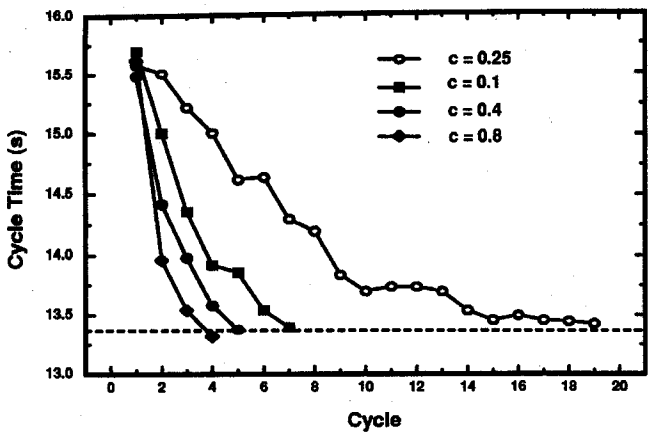

Fig. 13 Reduction in cycle time by RCB with different confidence levels

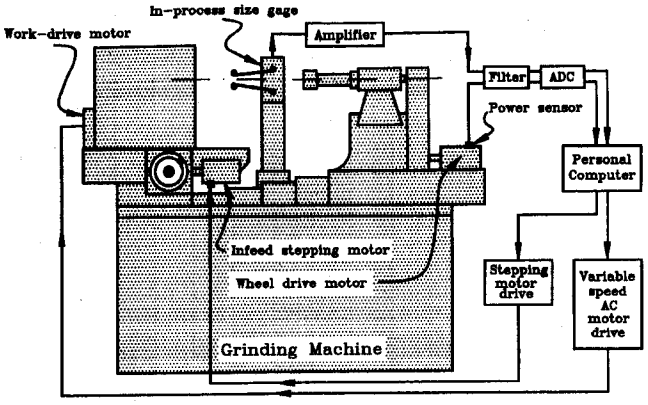

Fig. 15 Internal grinder retrofitted with a power monitor and size gage and interfaced to a personal computer

comes active for the last cycle, so no further reduction of the safety margin is possible without violation of this constraint.

Convergence of the cycle toward its minimum-time was also studied for three additional confidence levels: 0.10, 0.40 and 0.80. In Fig. 13, it can be seen that all the cycle-times approach the same minimum value represented by the dashed line, except for the highest confidence level of 0.80 which causes a constraint violation at the last cycle. The constraint violation in Fig. 13 presents an alternative view that the confidence level acts as the iteration step size. The point that too high an iteration step (confidence level) could lead to too steep a convergence rate and a missed ultimate target can be better viewed through the values of remaining infeed and depth of burn for three of the last cycles at the confidence level of 0.80 in Fig 14. Just as shorter cycle-times are achieved by bringing the depth of burn values closer to the remaining infeed, failed cycles are generated when the depth of burn exceeds the remaining infeed during the cycle.

4 Experimental Results

The optimal infeed control strategy was implemented on a Bryant Model No. 1116 Internal Grinder (see Fig. 15) interfaced to a micro-computer for process control and data acquisition [6]. The machine is retrofitted with a stepper motor infeed drive, an electrical workpiece drive, a power monitor (A.F. Green TT2), and an in-process size gauge (Marposs Micromar 5 and E9 amplifier). Experiments were conducted using a 32A80J7VBE wheel of diameter $d_s = 50$ mm to grind a hardened AISI 52100 bearing steel (HRC=62) of internal diameter $d_w = 70$ mm across its entire 9 mm width while applying a 5% solution of water soluble fluid. For all these experiments, the peripheral wheel velocity was $v_s = 37$ m/s corresponding to a rotational wheelspeed of $n_s = 14{,}000$ rpm, and the peripheral workpiece velocity was $v_w = 1.1$ m/s corresponding to a rotational workspeed of $n_w = 300$ rpm. The wheel was dressed before each cycle using a single point diamond with the dressing lead s_d selected so as to satisfy the surface roughness requirement according to the relationship [2]:

$$s_d = \left[\frac{R_a}{R_0}\left(\frac{v_s}{\pi d_w v}\right)^{\gamma} a_d^{1/y}\right]^{1/x} \tag{10}$$

where R_0, x, y and γ are empirical constants. The dressing depth a_d was set at 0.01 mm for all these tests. The maximum command infeed rate was used in place of the actual infeed rate v in Eq. (10) to satisfy the surface roughness requirement of $R_a = 0.7$ μm. The sampling period was set at 0.04 s so as to provide adequate computation time for control while allowing frequent enough state evaluations during the cycle.

In the first experiment, the maximum infeed rate was set as 0.026 mm/s, close to the upper allowable limit of the machine [6], and the time constant was approximated as 1.8 s. The command and actual infeed rates for this experiment are shown in Fig. 16. The controller produced only a two-stage cycle, apparently because the specified maximum allowable infeed rate was insufficient to cause enough thermal damage to require an intermediate section. This measured power remained below the estimated burning power as seen in Fig. 17. The observed power saturation was due to the limitation of the power monitor. This does not pose a

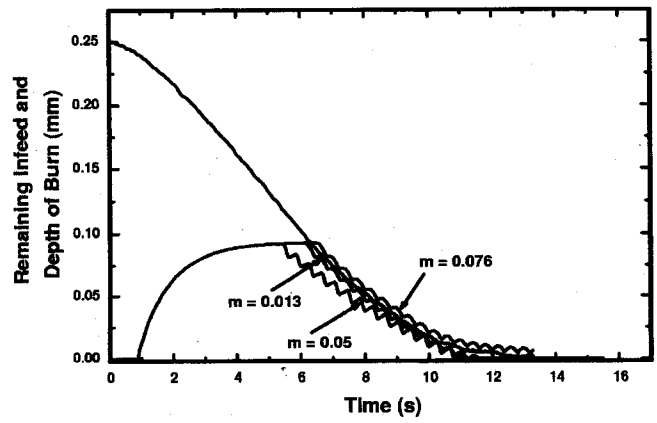

Fig. 14 Remaining infeed and depth of burn with different safety margins

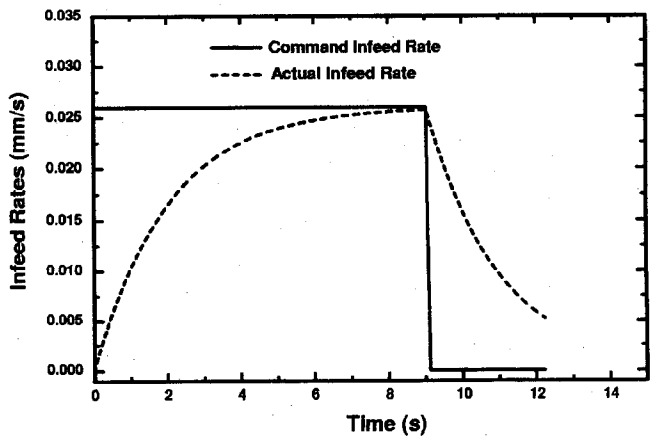

Fig. 16 Infeed rate profiles during the first experiment

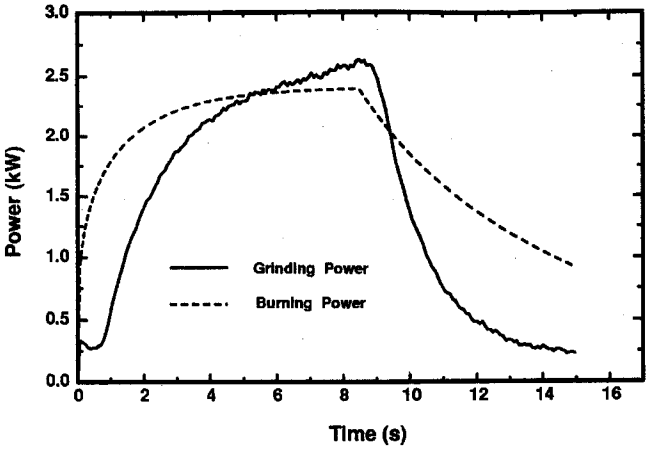

Fig. 17 Measured power and burning power during the first experiment

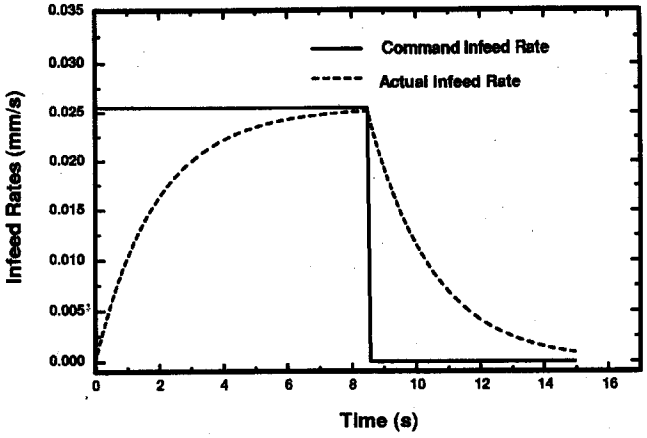

Fig. 19 Infeed rate profiles during the second experiment

constraint on the cycle, but it causes an erroneous estimation of the depth of burn. In this case, the intermediate section did not occur because the estimated depth of thermal damage never reached the remaining infeed, as seen in Fig. 18. As for the validity of the cycle, it can be seen from Fig. 16 that the final actual infeed rate is too high to satisfy the roundness constraint–the final roundness value is estimated at 3.9 μm which exceeds the roundness constraint of 3.0 μm. Violation of the roundness constraint is caused by insufficient spark-out due to under-estimation of the system time constant.

In order to avoid power saturation and to satisfy the roundness specification, the maximum allowable limit of the infeed rate for the next experiment was reduced to 0.0255 mm/s and the time constant was increased to 1.95 s as estimated from the first experiment. The infeed rate profiles for this experiment in Fig. 19 show a longer cycle due to the smaller allowable infeed rate and the need for a longer spark-out stage to accommodate the roundness specification. The final roundness value for this experiment was 2.9 μm, which was within the specification of 3 μm. The grinding power for this experiment shown in Fig. 20 was below the saturation limit of the power monitor. The optimal cycle-time obtained from the optimization strategy of Xiao and Malkin [6] for the conditions used in the experiments was 24.66 s, which is 38% longer than the cycle-time in the experiment.

It is apparent from these experimental results that accurate estimation of the time constant is an important factor for successful implementation of the control strategy. In some cases, it may not be possible to satisfy the roundness requirement if the estimated time constant is too big. As with wheel dullness, taking a conservative approach can protect the cycle from an erroneous time constant. A more conservative roundness requirement would force a longer spark-out stage until the time constant value can be updated through post-cycle adaptation. However, for practical implementation of this control strategy relationships for surface roughness, roundness and depth of burn are needed, which are dependent on the material properties and the machine.

5 Conclusions

A system was developed and implemented for optimal on-line control of grinding cycles with continuously variable infeed rates. In the first part of this study it was found that optimal grinding cycles should consist of distinct segments with predominant constraints [1]. The control system was developed to identify the state of the cycle from the measurements of size and power, and to compute the infeed rate according to the dominant constraint. The control system relies on the process model for its performance, and therefore is affected by modeling inaccuracies. Feedback measurements of size and power provide some compensation for modeling inaccuracy, but they do not ensure seamless implementation of the controller. Two of the safeguards included in the controller are a safety margin to incorporate conservatism into the model and parameter estimation to update the critical parameters based on measurements of power and size. The control system was successfully implemented on an internal cylindrical grinding machine, which resulted in a cycle-time considerably shorter than a corresponding traditional cycle.

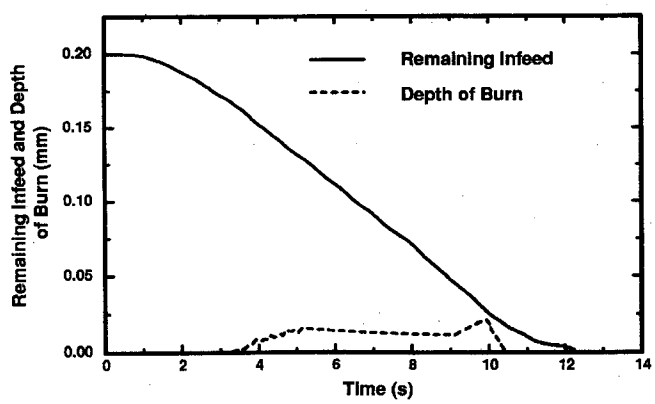

Fig. 18 Remaining infeed and depth of burn during the first experiment

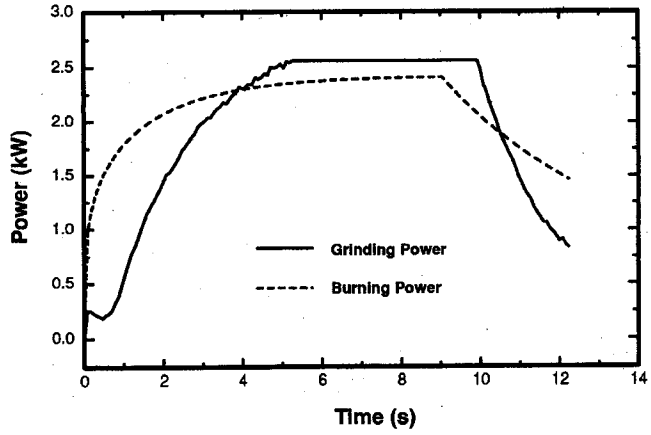

Fig. 20 Measured power and burning power during the second experiment

Acknowledgment

This research was supported by NSF Grant No. DMI-9908070.

References

[1] Dong, S., Danai, K., Malkin, S., and Deshmukh, A., 2003, "Continuous Optimal Infeed Control for Cylindrical Plunge Grinding-Part 1: Methodology," ASME J. Manuf. Sci. Eng., **125**, pp. 327–333.

[2] Malkin, S., 1989, *Grinding Technology: Theory and Applications of Machining with Abrasives*, Society of Manufacturing Engineers, Detroit, Michigan.

[3] Chiu, N., and Malkin, S., 1993, "Computer Simulation for Cylindrical Plunge Grinding," CIRP Ann., **42**(1), pp. 383–387.

[4] Chiu, N., 1989, "Computer Simulation for Cylindrical Plunge Grinding," M. S. Thesis, University of Massachusetts Amherst.

[5] Ivester, R., Danai, K., and Malkin, S., 1997, "Cycle Time Reduction in Machining by Recursive Constraint Bounding," ASME J. Manuf. Sci. Eng., **119**(2), pp. 201–207.

[6] Xiao, G., and Malkin, S., 1996, "On-Line Optimization of Internal Cylindrical Grinding Cycles," CIRP Ann., **45**(1), pp. 287–292.